Elimination of the error signal in the superior colliculus impairs saccade motor learning

Yoshiko Kojima[a,1] and Robijanto Soetedjo[a,b]

[a]Washington National Primate Research Center, University of Washington, Seattle, WA 98195-7330; and [b]Department of Physiology and Biophysics, University of Washington, Seattle, WA 98195-7330

Edited by Michael E. Goldberg, Columbia University College of Physicians, New York, NY, and approved August 8, 2018 (received for review April 11, 2018)

When movements become dysmetric, the resultant motor error induces a plastic change in the cerebellum to correct the movement, i.e., motor adaptation. Current evidence suggests that the error signal to the cerebellum is delivered by complex spikes originating in the inferior olive (IO). To prove a causal link between the IO error signal and motor adaptation, several studies blocked the IO, which, unfortunately, affected not only the adaptation but also the movement itself. We avoided this confound by inactivating the source of an error signal to the IO. Several studies implicate the superior colliculus (SC) as the source of the error signal to the IO for saccade adaptation. When we inactivated the SC, the metrics of the saccade to be adapted were unchanged, but saccade adaptation was impaired. Thus, an intact rostral SC is necessary for saccade adaptation. Our data provide experimental evidence for the cerebellar learning theory that requires an error signal to drive motor adaptation.

motor learning | error signal | saccade | superior colliculus | cerebellum

When movements are inaccurate, the brain detects the error, i.e., the distance remaining between the goal and the end point of the actual movement, and adjusts subsequent movements to reduce the error. This process is called motor adaptation or motor learning. A cerebellar learning theory (1–3) suggests that a motor error increases the complex spike activity of Purkinje cells (P cells). This weakens the synaptic strength of the parallel fiber input to P cells, which in turn decreases their simple spike activity. The altered simple spike activity then is delivered via a cerebellar nucleus to the brainstem or elsewhere where it adjusts erroneous motor commands.

Previous studies tried to prove that an error signal to the cerebellum is required to induce motor learning. For example, for adaptation of the vestibular ocular reflex (4–8) and eye blink/fear conditioning (9–15), inactivation of the inferior olive (IO), the origin of the climbing fibers that produce complex spikes, somewhat impaired the learning. However, these results are inconclusive because inactivation of the IO also affected the movement itself (4–16). In the experiments that selectively eliminated the error signal by blocking a receptor of the error signal in the IO (17) or by suppressing the complex spike activity behaviorally (18), the movement itself was not affected, but neither was the learning. Thus, it is currently unclear whether an error signal to the cerebellum is required to induce motor learning. In this study, we selectively eliminated an error signal to the IO at its source, a strategy that did not affect the movement to be adapted.

Saccadic eye movements provide an excellent model to study the neuronal mechanisms of motor adaptation because the basic circuitry for saccade generation is well known (19). Also, it is possible to induce an apparent error by displacing the target during a saccade so the saccade appears to have fallen short or to have overshot (20). If the error persists over many trials, the saccadic system gradually adjusts the signal that is producing the faulty saccade so the saccade lands closer to the displaced target. A recent body of research suggests that the cerebellum plays an important role in saccade adaptation. First, patients with cerebellar disorders cannot undergo saccade adaptation (21, 22). Second, large excisions or pharmacological manipulations of the oculomotor vermis (OMV), a saccade-related area of the cerebellar cortex, impair adaptation (23–26). Finally, consistent with the learning theory mentioned earlier, the probability of complex spike occurrence in the OMV increases, and the firing rate of simple spikes decreases during saccade adaptation (refs. 27–30, cf. refs. 31 and 32).

The superior colliculus (SC) produces a saccade motor command signal (19). In addition, previous studies have implicated the SC as the source of the error signal that drives saccade adaptation. First, there are disynaptic routes from the SC to the OMV. The climbing fibers that cause complex spikes in OMV P cells originate in the part of the inferior olive (33, 34) that receives a projection from the SC (35, 36). Second, stimulation of the rostral SC timed to occur when complex spike enhancement during saccade adaptation would normally take place actually produces saccade adaptation without any natural visual error (37, 38). This finding suggests that SC stimulation can act as a surrogate error signal to drive adaptation, presumably by evoking complex spikes in the OMV. Finally, the visual activity of rostral SC neurons is correlated with the speed of saccade adaptation; that is, SC activity was strongest when the rate of adaptation was fastest (39). All these studies taken together suggest that the SC could provide an error signal to the OMV through the IO to drive saccade adaptation. Thus, we can eliminate the error signal that drives saccade adaptation by inactivating the rostral SC. If this SC-elicited error signal is not only sufficient but necessary to induce saccade adaptation, SC inactivation should impair this type of motor learning.

Significance

Theories of cerebellar-dependent motor learning use the error between the desired and actual movement to correct the erroneous movement. To support this idea, several studies have tried to eliminate the error signal to the cerebellum and demonstrate an impairment of learning. However, such former approaches have not been successful because blocking the error signal also affected the movement to be learned. In this study, we selectively block an error signal for saccade adaptation, a type of cerebellar motor learning, by inactivating the source of the error signal in the superior colliculus without affecting the movement to be learned. Saccade adaptation was impaired. Thus, our study provides the first experimental evidence that an error signal is required for cerebellar motor learning.

Author contributions: Y.K. and R.S. designed research; Y.K. performed research; Y.K. analyzed data; and Y.K. wrote the paper.

The authors declare no conflict of interest.

This article is a PNAS Direct Submission.

[1]To whom correspondence should be addressed. Email: ykojima@u.washington.edu.

This article contains supporting information online at www.pnas.org/lookup/suppl/doi:10.1073/pnas.1806215115/-/DCSupplemental.

Published online September 5, 2018.

Results

We tested the consequences of unilateral muscimol injections into the rostral SC on saccade adaptation in six experiments. Because SC neurons are organized topographically (40), we identified the preferred vector at the injection site by microelectrical stimulation through the injectrode (Fig. 1*A*) (see *Materials and Methods* for further details). The details of those experiments, including the participating monkey, the amount of the drug injected, the side of the injection, and the preferred vector at the injection site, are presented in Table 1.

Each injection experiment consisted of three blocks: preinjection, postinjection, and adaptation (see *Materials and Methods* for detail). During preinjection and postinjection blocks, the monkey made visually guided saccades to three target steps of either (*i*) the injection site's preferred vector (visual error vector; green arrow in Fig. 1*A*), (*ii*) 10° in the preferred vector direction (preferred bigger vector; blue arrow in Fig. 1*A*), or (*iii*) 15° opposite to the preferred direction (adapt saccade vector; red arrow in Fig. 1*A*). Each target step occurred randomly, so the starting position of each saccade was random. Once we collected the preinjection data for at least 5 min, we injected muscimol and collected postinjection data for at least 15 min to confirm that the muscimol affected saccades to the visual error vector but not saccades to the adapt saccade vector. Then we began the adaptation. In this adaptation block, we evoked gain decrease adaptation of the adapt saccade vector (red arrow in Fig. 1*B*) by presenting a backward intrasaccadic target step equal to the visual error vector (green arrow in Fig. 1*B*). Because the directions of the adapt saccade vector and the visual error vector are opposite, this combination induces a gain decrease adaptation. For the preferred bigger vector, we also presented the visual error vector as an intrasaccadic target step. However, in this case, because the preferred bigger vector (blue arrow in Fig. 1*B*) and the visual error vector (green arrow in Fig. 1*B*) are in the same direction, this combination produced an increase in saccade size. We kept the postsaccadic visual error constant during the entire adaptation session (green arrow in Fig. 1*B*, late adaptation) to keep the SC area representing the visual error within the inactivated SC area during adaptation (*Materials and Methods*).

Effect of Muscimol Injection on Saccades. Consistent with the previous studies (41–45), muscimol injections into the SC strongly affect contraversive saccades whose vector is represented within the inactivated area but only modestly affect ipsiversive saccades. Fig. 2*A* shows the gain of saccades whose target vector was congruent with the vector of the inactivated area (visual error vector, Fig. 1*A*, green arrow). The median gain of the first 25 preinjection saccades was 0.94 (Fig. 2*A*, left box). The median gain of the last 25 postinjection saccades (0.78; Fig. 2*A*, right box) was significantly smaller (Wilcoxon rank sum test, $P = 1.4 \times 10^{-4}$). The median reaction time of the primary saccade increased significantly after the injection from 195.1 to 385.4 ms (Fig. 2*B*; preinjection, 195.1 ms; postinjection, 385.4 ms; Wilcoxon rank sum test, $P = 1.8 \times 10^{-7}$). On the other hand, the gain of 15° ipsiversive saccades (adapt saccade vector, Fig. 1, red arrow) did not change (Fig. 2*C*; preinjection, 1.00; postinjection, 1.02; Wilcoxon rank sum test, $P = 0.18$). The variability of the gain was slightly increased (Fig. 2*C*; interquartile range; preinjection, 0.044; postinjection, 0.083). The reaction time decreased slightly from 161.1 to 146.9 ms (Fig. 2*D*; Wilcoxon rank sum test, $P = 5.2 \times 10^{-3}$).

Data from all six experiments are summarized in Fig. 3. Fig. 3*A* shows the gain of the saccades used as visual error vectors. In all six experiments, the median gain of the last 25 postinjection saccades was significantly smaller than that of the first 25 preinjection saccades. Thus, we confirmed that the muscimol injection effectively suppressed the activity of the SC site whose vector was to be used as the visual error to induce adaptation.

Fig. 3*B* shows the gain of saccades used for gain decrease adaptation (adapt saccade vectors). None of the six experiments showed a significant difference between the median gain of the first 25 preinjection saccades and the last 25 postinjection saccades. Thus, the muscimol injection did not affect the gain of the ipsiversive 15° saccades that were to undergo gain decrease adaptation.

Fig. 3*C* shows the gain of saccade used for gain increase adaptation (preferred bigger vector). The gain did not change significantly in half of the six experiments. We selected these three experiments to analyze gain increase adaptation.

Effect of Muscimol Injection on Gain Decrease Adaptation. Fig. 4 shows the course of the gain change during adaptation from representative datasets 1 and 6. Each dataset consists of one injection and three control experiments. The exponential fit of the course of adaptation after the injection (black line) showed either a slower gain decrease (Fig. 4*A*) or a slight gain increase (Fig. 4*B*). In contrast, the three associated control experiments showed robust gain decreases (gray lines). For both datasets, the fits for the injection experiment were significantly different from those of any of the three associated control experiments (gray solid and dashed lines in Fig. 4 *A* and *B*; $P < 0.0001$ for injection vs. all controls in both datasets) (*Materials and Methods*).

The variability of the gain of the last 25 saccades during adaptation was slightly larger in the injection experiment than in the control experiments (Fig. 4, interquartile range; dataset 1, injection, 0.11; controls, 0.053, 0.090, 0.062; dataset 6, injection, 0.079; controls, 0.065, 0.052, 0.063).

Table 1. Summary of the conditions in all six injection experiments

Exp. no.	Monkey	SC	Preferred vector		Muscimol (μL)
			Direction	Amplitude	
1	Z	Right	185	6	1
2	Z	Left	330	2	0.8
3	Z	Right	186	7.5	1
4	D	Left	30	4	1
5	D	Right	141	5.5	1.2
6	D	Left	353	2.3	1

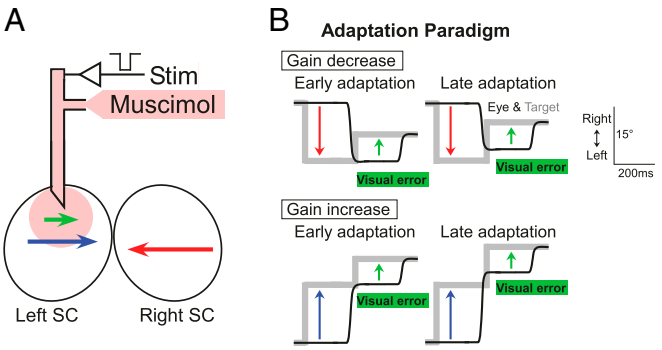

Fig. 1. Injection and adaptation procedures. (*A*) Muscimol injection into the rostral SC. A 35-gauge epoxylite-insulated stainless steel tube delivers microstimulation to evoke a saccade and muscimol to inactivate that portion of SC (pink). Green arrow represents the injection site's preferred vector, called the visual error vector. Blue arrow shows a 10° vector in the preferred vector direction (preferred bigger vector); red arrow represents a 15° vector in the nonpreferred direction (adapt saccade vector). A unilateral injection inactivates the visual error vector (green arrow) but does not affect the adapt saccade vector (red arrow), which is represented in the other SC. (*B*) The intrasaccadic adapt target step is held constant at the visual error vector. Target step vectors (red, blue, and green arrows) used in the constant error paradigm are the same as those in *A*.

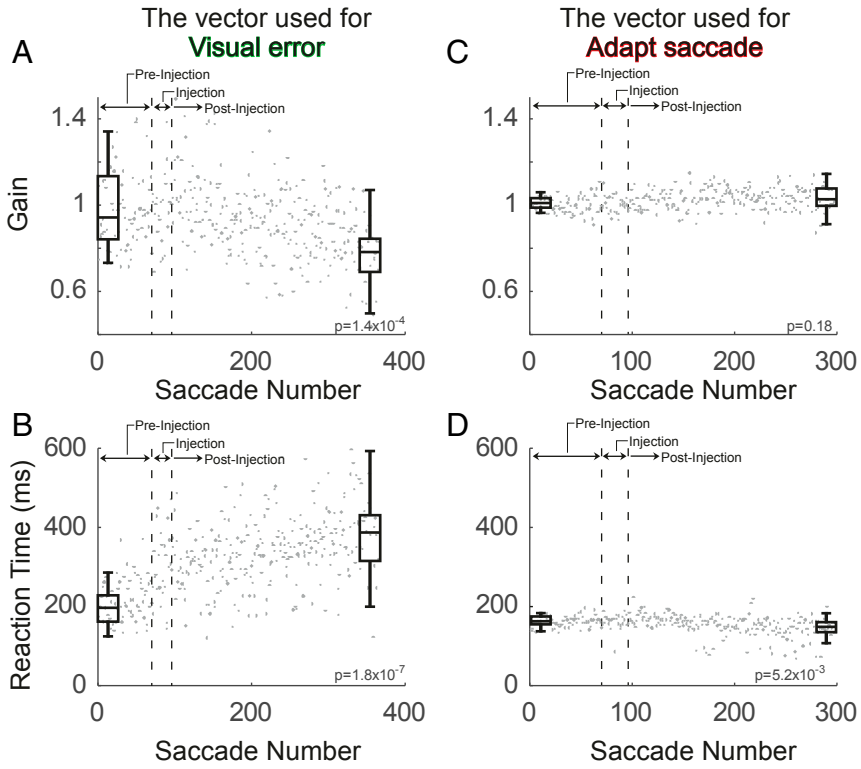

Fig. 2. Effect of muscimol on saccades congruent with the (*A* and *B*) visual error vector and (*C* and *D*) adapt saccade vector in injection experiment 1 (Exp. 1 in Table 1). (*A* and *C*) Time course of gain change before, during, and after the injection but before the adaptation session. (*B* and *D*) Time course of reaction time before, during, and after the injection but before the adaptation session. Each dot indicates a saccade. Box plots indicate the first and last 25 saccades of preinjection and postinjection, respectively. For the visual error vector, the injection produced a significant change in both saccade gain (*A*) and reaction time (*B*). For the adapt saccade vector, the reaction time was slightly decreased (*D*), but the gain was unchanged (*C*).

Fig. 5 shows the amount of gain change, i.e., the difference between the median gains of the first and last 25 saccades of adaptation (*Materials and Methods*). In dataset 1, the gain change after the injection was −0.0028, which was not significantly different from 0 (Fig. 5, dataset 1, black bar) (Wilcoxon rank sum test, first vs. last 25 saccades, $P = 0.95$). In contrast, the gain changes in the three control experiments, −0.09, −0.13, and −0.14, were all significantly different from 0 (Fig. 5, dataset 1, gray bars) (Wilcoxon rank sum test, first vs. last 25 saccades, $P = 1.6 \times 10^{-5}$, 1.2×10^{-5}, and 1.2×10^{-5}, respectively). In the remaining five datasets, the gain change during adaptation in the injection experiment also was not significant (Fig. 5, black bars). However, the control adaptations associated with datasets 2 through 6 all exhibited significant gain changes (Fig. 5, gray bars). In some injection experiments (2, 3, 5, and 6), the gain increased slightly during the gain decrease paradigm, but the changes were not significantly different from 0. Thus, inactivation of the rostral SC prevented the gain decrease that normally occurs during behavioral adaptation.

Finally, we examined the saccade peak velocity and duration during gain decrease adaptation. Because the saccade amplitude during an injection experiment did not change during adaptation, we anticipated that other saccade metrics also would not change. Fig. 6*A* shows the peak velocity during adaptation in dataset 1. The median velocities of the first and last 25 saccades (626.7°/s and 624.7°/s, respectively) were not significantly different in the injection experiment (Wilcoxon rank sum test, $P = 0.95$) (black circles and line). For each of the three control experiments, the median of the last 25 saccades was significantly lower than that for the first 25 saccades (Wilcoxon rank sum test, $P = 0.0038$, 0.0011, and 0.0070, for control 1, 2, and 3, respectively) (gray circles and lines) because the amplitude had decreased during adaptation (46). The duration was not significantly different in either the injection experiment or any of the three control experiments (Fig. 6*B*; Wilcoxon rank sum test, $P = 0.84$, 0.83, 0.38, and 0.51 for injection and control 1, 2, and 3, respectively).

Fig. 6 *C* and *D* compare the median values of the first and the last 25 saccades of adaptation from all six injection experiments. None of the injection experiments showed a significant change in saccade peak velocity (Wilcoxon rank sum test, $P > 0.05$) (Fig. 6*C*), and there was no consistent change in the

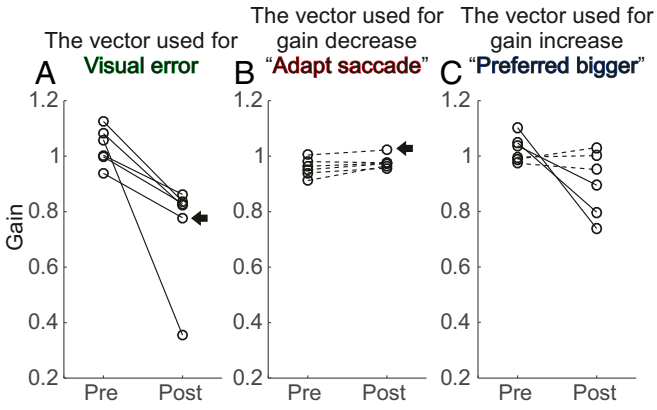

Fig. 3. Effect of muscimol on saccades congruent with (*A*) the visual error vector, (*B*) the adapt saccade vector, and (*C*) preferred bigger vector for all six injection experiments. Circles show the median of the first and last 25 saccades of preinjection and postinjection, respectively. Solid and dashed lines indicate whether the first and last medians, respectively, are significantly different or not. Arrows indicate data from experiment 1 in Fig. 2.

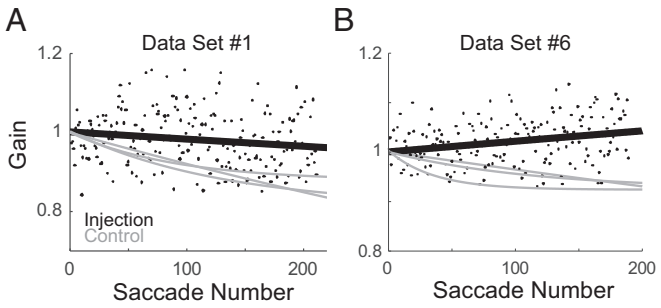

Fig. 4. Gain change during adaptation for datasets (*A*) 1 and (*B*) 6. Black dots represent individual saccades, and black lines are exponential fits for the injection data. Gray lines are exponential fits for the three associated control experiments. The exponential fits for the injection and associated control datasets are significantly different.

population of six experiments (Wilcoxon signed rank test, $P = 0.31$). Also, saccade duration did not change significantly in any of the six injection experiments (Wilcoxon rank sum test, $P > 0.05$) (Fig. 6*D*), and there was no consistent change in the population of six experiments (Wilcoxon signed rank test, $P = 0.84$). Thus, the injection did not change any of the saccade metrics during adaptation.

Fig. 6 *E* and *F* summarize the data from all 18 control experiments. Most of the experiments (14/18, 78%) showed a significant change in peak velocity (Wilcoxon rank sum test, $P < 0.05$) (Fig. 6*E*), and it was consistent in the population (Wilcoxon signed rank test, $P = 0.0002$). Most of experiments (14/18, 78%) showed no significant change in saccade duration (Wilcoxon rank sum test, $P > 0.05$) (Fig. 6*F*), and there was no consistent change in the population (Wilcoxon signed rank test, $P = 0.79$). Thus, consistent with the previous study (46) and as expected from their amplitude–velocity relation (47), peak velocity decreased during control adaptations because saccade amplitude decreased.

Effect of Muscimol Injection on Gain Increase Adaptation. Fig. 7 shows the amount of gain change for contraversive saccades that were examined during gain increase adaptation. We selected three experiments in which the muscimol injection did not affect the gain of the contraversive saccades to be adapted (Fig. 3*C*). In dataset 4, the gain change after the injection was −0.022, which was not significantly different from 0 (Fig. 7, dataset 4, black bar) (Wilcoxon rank sum test, first vs. last 25 saccades, $P = 0.08$). In contrast, the gain changes in the three associated control experiments, 0.040, 0.031, and 0.026, were all significantly different from 0 (Fig. 7, dataset 4, gray bars) (Wilcoxon rank sum test, first vs. last 25 saccades, $P = 3.3 \times 10^{-4}$, 4.0×10^{-2}, and 9.0×10^{-3}). In the remaining two datasets, the gain change during adaptation in the injection experiment also was not significant (Fig. 7, black

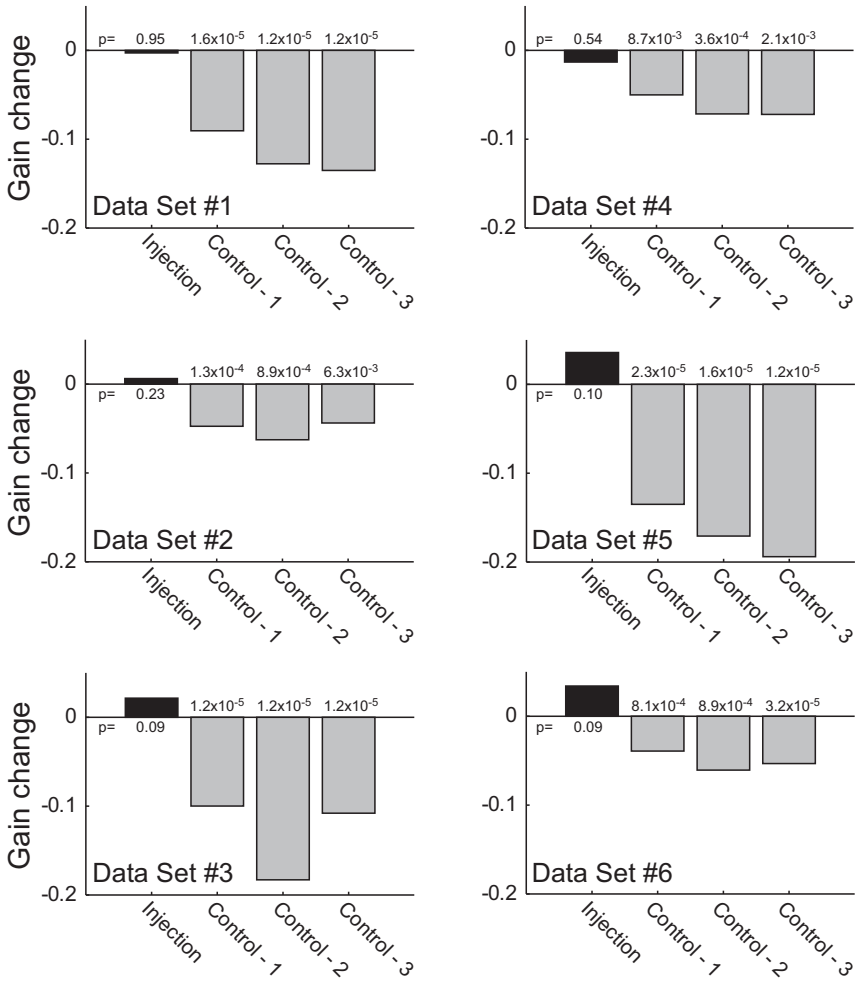

Fig. 5. Gain change during gain decrease adaptation for all six datasets. Black bars indicate the injection experiments; gray bars indicate the three control experiments associated with each injection. None of the injection experiments exhibited a significant gain change, whereas all of the control experiments did.

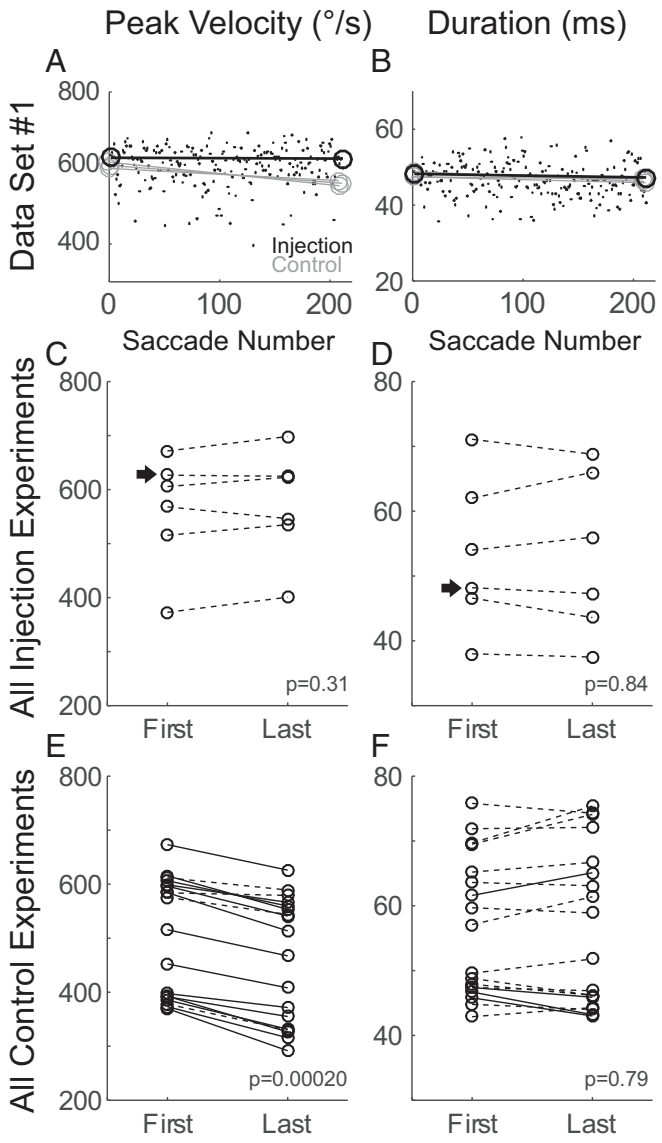

Fig. 6. Changes in saccade (*A*, *C*, and *E*) peak velocity and (*B*, *D*, and *F*) duration during adaptation. (*A* and *B*) Time course of the changes during adaptation in dataset 1. Black dots represent individual saccades in the injection experiment. Black circles are the median of the first and last 25 saccades. Gray circles are medians of the first and last 25 saccades of three associated control experiments. Summary of all (*C* and *D*) injection experiments and (*E* and *F*) control experiments. Circles are the medians of the first and last 25 saccades of each experiment. Solid and dashed lines indicate whether the first and last medians, respectively, are significantly different or not. None of the injection experiments were associated with a significant change in peak velocity (*C*), whereas most control experiments were (*E*). No injection experiment (*D*) and most of the control experiments (*F*) were not associated with significant changes in saccade duration.

bars). However, the control adaptations associated with datasets 5 and 6 all exhibited significant gain increases (Fig. 7, gray bars). Thus, inactivation of the rostral SC prevented the gain increase that normally occurs during behavioral adaptation.

Discussion

Our study shows that an error signal originating in the rostral SC is required for saccade adaptation, a type of cerebellar motor learning (21–30, 48, 49). We inactivated the rostral SC because it provides an input to the IO climbing fiber origin of the error signal that drives saccade adaptation (33–39). We first confirmed that rostral SC inactivation affected only the error vector but not the vector of saccades to be adapted (Figs. 2 and 3). Then, we showed that saccade gain (Figs. 4 and 5) and its other metrics, i.e., peak velocity and duration (Fig. 6), were not changed in any experiment. Thus, elimination of the error signal from the SC affected saccade adaptation specifically and no other saccade metrics. Therefore, this error signal is required for saccade adaptation to occur.

Possible Concerns About Our Conclusions.

Small changes in primary saccade characteristics. Unilateral SC inactivation did not change the amplitude (Fig. 3*B*), peak velocity (Fig. 6*C*), or duration (Fig. 6*D*) of the ipsiversive primary saccade to be adapted because that saccade is controlled by the opposite SC. However, as shown in Fig. 2 and previous studies (41, 42, 44), inactivation slightly decreased saccade reaction time (Fig. 2*D*) and slightly increased the variability of the amplitude of the primary saccade (Fig. 2*C*). Do these modest changes possibly impair adaptation? Because the adaptation speed of express and targeting saccades is not significantly different in either monkeys (50) or humans (51), it is unlikely that the

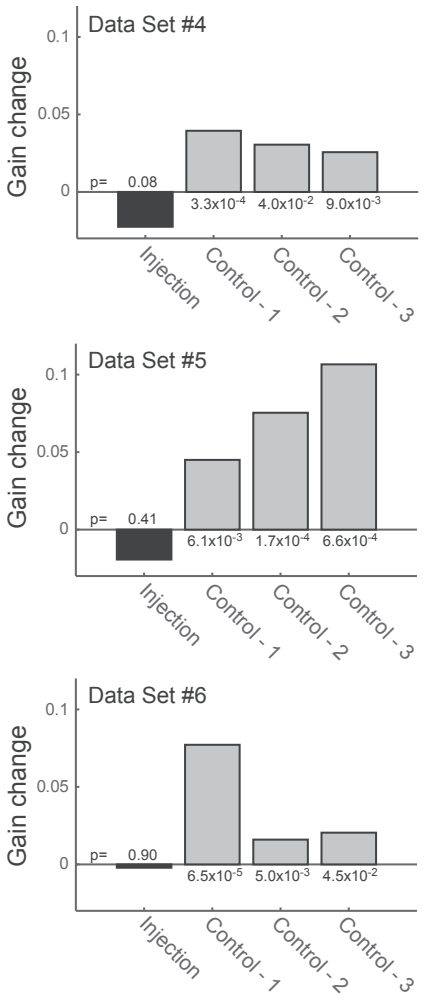

Fig. 7. Gain change during gain increase adaptation for three selected datasets. Black bars indicate the injection experiments; gray bars indicate the three control experiments associated with each injection. None of the injection experiments exhibited a significant gain change, whereas all of the control experiments did.

shortening of the reaction time impaired adaptation in our study. Moreover, in this study, although the reaction time of postinjection saccades was shorter than that of preinjection saccades, it was not as short as that of express saccades. How about the increase in saccade variability? If we had used the conventional adaptation paradigm (20), the variability of primary saccade amplitude would possibly reverse the sign of the error, which could slow the adaptation. In this study, however, we used a constant error adaptation paradigm (*Materials and Methods*), so this possibility could not account for our results. Therefore, the impairment of adaptation was not caused by a direct effect of muscimol on the primary saccade to be adapted.

Nystagmus. After the injection, nystagmus emerged in the later part of the adaptation session. It probably was caused by the spread of muscimol to the nucleus of the optic tract, which is located immediately rostral to the SC (44, 52–54). We stopped analyzing data as soon as nystagmus appeared (*Materials and Methods* and *SI Appendix*, Fig. S1).

Number of saccades. The stoppage of data analysis when nystagmus appeared did not cause a severe shortage of saccades to analyze. We always compared the same number of trials for an injection and its control experiments. As shown in Fig. 5, all control experiments exhibited a significant gain change. Therefore, the number of trials was sufficient to detect a normal speed of gain change during adaptation. However, if an adaptation were unusually slow requiring more trials to evolve, a low number of trials might not demonstrate a significant change. Therefore, our data could not distinguish whether adaptation was completely abolished or extremely slowed. However, this caveat does not change our conclusion that an SC error signal is required to drive a normal saccade adaptation.

Gain decrease and increase adaptations. Gain decrease adaptation has been tested for ipsiversive saccades and gain increase adaptation for contraversive saccades (Fig. 1). Because ipsiversive saccades are encoded in the SC opposite to the injection site, the muscimol injection did not affect the gain of the ipsiversive saccades (Fig. 2*B*). This made the interpretation of the muscimol effect on gain decrease adaptation clear; that is, the muscimol inactivation impaired the adaptation without affecting the movement itself. On the other hand, the effect of muscimol on contraversive saccades was not consistent; that is, muscimol affected the gain in half of experiments (Fig. 2*C*). Because contraversive saccades are encoded in the caudal SC on the side of the injection, the muscimol might have spread caudally in these experiments. Therefore, to analyze the gain increase adaptation of contraversive saccades, we selected the three experiments in which the gain of the contraversive saccades was not changed after the injection. In these three, the gain increase adaptation was impaired. Therefore, we conclude that an SC error signal is required to drive both amplitude decrease and increase adaptations.

Comparison with Previous Studies.

Saccade adaptation. Fig. 8 shows a simplified saccade block diagram to demonstrate the paths of two signals, i.e., **a** motor command signal and an error signal, from each side of the SC for adaptation of leftward saccades due to a rightward error (backward adaptation). The right SC produces a leftward saccade motor command that reaches contralateral motoneurons (MN) in the abducens nucleus via the brainstem burst generator (BG) (dark blue pathway in Fig. 8). This SC signal also reaches the oculomotor cerebellum (OMV) (cyan pathway) via the Nucleus Reticularis Tegmenti Pontis (NRTP). During adaptation, the SC motor command signal does not change (55, 56), suggesting that the adaptation site of the plastic change is downstream of the SC.

The results of this and other previous studies (37–39) indicated that in this situation, the left SC provides an error signal to the OMV through the IO (33–36) (red pathway) to drive adaptation. As suggested in a cerebellar learning theory (1–3), this error signal increases complex spike activity, which induces plastic changes that reduce simple spike activity (27–30) in the OMV (gray downward arrow next to OMV). This decrease in simple spike activity increases firing in cerebellar output neurons in the caudal fastigial nucleus (cFN) (57, 58), which, in turn, increases the activity of inhibitory burst neurons (IBN) (59) and decreases motoneuron activity (60) (purple pathway), which cooperate to reduce saccade size (backward adaptation). In this study, we suppressed the SC error signal (yellow X sign on red pathway), which prevented the plastic changes in the OMV, and saccade size remained essentially unchanged during behavioral adaptation (yellow X sign next to gray arrows).

The previous studies that examined the error signal in the SC used two approaches, i.e., stimulation (37, 38) and recording (39). Our laboratory and others electrically stimulated the rostral SC in the interval between the primary and corrective saccade (37, 38), i.e., when a visual error would occur during saccade adaptation (Fig. 1). This surrogate error signal caused adaptations with time courses like those induced by natural visual errors. Although these studies showed that stimulation of the rostral SC could simulate an error signal and drive saccade adaptation, it was unclear what aspect of the error signal SC neurons encoded. When we recorded the visual activity of rostral SC neurons during amplitude decrease adaptations produced by a constant error adaptation paradigm, it was correlated with the speed of adaptation. This suggests that the strength of SC activity controls adaptation speed (39). In our current inactivation experiment, we have shown that this SC signal

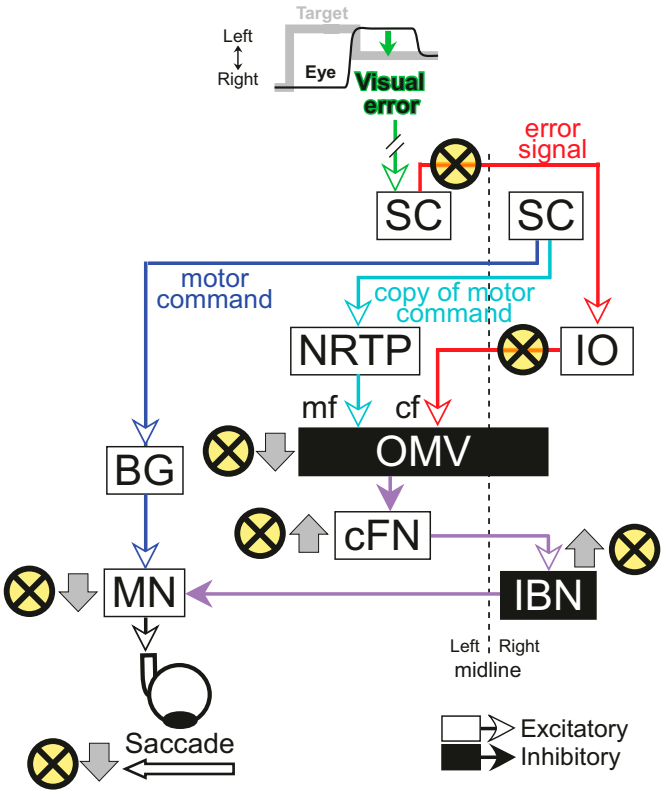

Fig. 8. Schematic of saccade neural circuits and changes that occur there during adaptation. Gray arrows indicate the changes in neural activity during gain decrease adaptation. Yellow and black X marks indicate that the plastic changes in the OMV no longer occur after a muscimol injection into the SC eliminates the error signal. BG, saccade burst generator; *cf*, climbing fibers; cFN, caudal fastigial nucleus; IBN, inhibitory burst neuron; IO, inferior olive; mf, mossy fibers; MN, abducens motoneuron; NRTP, nucleus reticularis tegmenti pontis; OMV, oculomotor vermis; SC, superior colliculus.

does not just reflect the ongoing error characteristics but provides the actual drive necessary to produce adaptation. Thus, our data provide a causal link between the SC error signal and saccade adaptation and demonstrate that an intact SC is necessary for adaptation to occur.

Error signals in other motor systems. Interpretation of previous studies that inactivated the IO to eliminate the error signal to the cerebellum for other learning tasks is complicated because the inactivation impaired not only learning but also the movement itself. These include adaptation of the vestibular ocular reflex (4–8), smooth pursuit movements (16), and eye blink/fear conditioning (9–15). Although there were differences among the studies, inactivation of the IO abolished motor learning (14). However, IO inactivation not only eliminated the error signal but also altered cerebellar tonic activity (17, 61–63), which is maintained by a neuronal loop involving the IO (IO–cerebellar cortex–cerebellar nucleus) (64, 65). Therefore, IO inactivation caused not only learning deficits but also motor deficits, such as nystagmus, hypotonia, and deep depression of motor activity (14, 61). To avoid such direct influences on the movement itself, we affected the error signal before it had reached the IO. Indeed, saccade amplitude was not changed by our muscimol injection (Fig. 3*B*).

Three previous studies that attempted to block the error signal selectively were not successful in impairing motor learning. First, in eye blink conditioning, the sensory error signal is believed to be transmitted to IO neurons by glutamate (64–66), whereas GABAergic input from the deep cerebellar nucleus maintains the tonic activity. Therefore, in principle, injection of the glutamate blocker to the IO should eliminate the error signal selectively. However, the injection did not abolish conditioning of the eye blink (17). To examine the vestibular–ocular reflex (VOR) adaptation, complex spike activity was suppressed behaviorally (18). However, VOR adaptation was not abolished. The authors suggested that complex spikes are not necessary for VOR adaptation and that another instructive signal, for example, a change in simple spike activity, may be involved. Obviously, our SC inactivation might eliminate not only changes in complex spike activity but also another instructive signal, although we feel this is unlikely. Finally, to compromise the error slip signal that drives adaptation of smooth pursuit eye movement, the nucleus of the optic tract (NOT), a nucleus with visual slip activity that also projects to the IO, was inactivated (16). Because the inactivation of the NOT induced a nystagmus that affected smooth pursuit directly, the effect on adaptation was inconclusive. Our study shows an impairment of adaptation by selective elimination of the error signal that drives it without affecting the saccade to be learned.

Materials and Methods

Surgery and Training. Two male rhesus monkeys (Z and D, *Macaca mulatta*) participated in the study. We implanted each monkey with fixtures to prevent head movements; a scleral search coil (67) to measure eye position in space; and a recording chamber, which was aimed at the midline between the two SCs.

After the monkeys had recovered from the surgery, we trained them to track a small visual target in a dimly lit, sound-attenuating booth. The monkey sat in a primate chair with its head restrained. We measured eye position with the electromagnetic search coil method (68) and rewarded the monkeys with applesauce for keeping their gaze within ±2° windows around the horizontal and vertical positions of the target spot continually for at least 0.5 s. Once they were trained to fixate the target spot, we trained them to make visually guided saccades to a stepping spot that moved to random locations on a tangent screen within ±18° of straight-ahead. We delivered the applesauce reward (~0.16 mL per dollop, ~200 mL/h) by a pump (masterflex tubing pump; Cole–Parmer) every 2 s regardless of the amplitude, direction, or timing of the saccade as long as it landed within the ±2° window surrounding the target. The targeting saccade was required to occur within 0.6 s of the target step, and the subsequent fixation had to be maintained for at least 0.3 s. The target was a 0.3° laser spot projected onto a tangent screen via two computer-controlled orthogonal mirror galvanometers. The screen was 65 cm from the monkey's eyes.

After the monkey reliably tracked the jumping target spot, we started recording and electrical stimulation experiments to delineate the SC topographic map (40, 69, 70). We used a glass-coated tungsten microelectrode (Alpha–Omega) guided by a 21-gauge hypodermic cannula.

All experiments were performed in accordance with the *Guide for the Care and Use of Laboratory Animals* (71) and exceeded the minimal requirements recommended by the Institute of Laboratory Animal Resources and the Association for Assessment and Accreditation of Laboratory Animal Care International. All of the procedures were evaluated and approved by the local Animal Care and Use Committee of the University of Washington.

Injection Procedure. We injected muscimol (5 μg/μL; MP Biomedicals) dissolved in a saline solution through a 35-gauge stainless steel tube that was insulated by epoxylite except for its beveled tip to allow the recording of background activity and electrical stimulation. On the day preceding each injection, we made electrode penetrations to locate the SC and to reveal the optimal vector of that locus (39, 69, 70, 72, 73) by recording and stimulation (50 μA, 500 Hz, 50-ms trains of 0.1-ms cathodal pulses). On the day of the injection, we advanced the injection tube until we heard neuronal bursts related to pseudorandom (in direction and size) target steps and/or the targeting saccades. We then stimulated five times via the same tube to evoke saccades. We identified the site's preferred vector by averaging the vectors of the five evoked saccades. The preferred vectors of the six injection sites are indicated in Table 1. Because stimulation of the rostral SC induces greater adaptation than stimulation of the caudal SC (37, 38), we tried to inject into the rostral SC, whose neurons respond best to small target eccentricities and/or saccade amplitudes (40). The range of the preferred amplitudes at our six injection sites was 2.0–7.5° with a median of 4.0° (Table 1). After we collected a preinjection block of saccades (see below), we injected the muscimol by using brief pulses of air pressure (PV830 Pneumatic PicoPump; World Precision Instruments).

Experimental Procedures. In each injection experiment, we first collected at least 5 min of preinjection data. During this block, the monkey made visually guided saccades to target steps of either (*i*) the site's preferred vector (visual error vector; green arrow in Fig. 1*A*), (*ii*) 10° in the preferred vector direction (preferred bigger vector; blue arrow in Fig. 1*A*), or (*iii*) 15° opposite to the preferred direction (adapt saccade vector; red arrow in Fig. 1*A*). The three target steps occurred at random, so the starting position of each saccade was random. After we had collected the preinjection data, we injected 800 nL of muscimol and monitored the reaction time of the saccades with the preferred vector while the monkey performed the same task. We added 200 nL every 5 min until the reaction time of saccades to the visual error vector increased. We collected at least 15 min of postinjection data for the same tasks.

After collecting the postinjection data, we started the adaptation. In this adaptation block, we caused adaptation of the adapt saccade vector (red arrow in Fig. 1 *A* and *B*) and preferred bigger vector (blue arrow in Fig. 1*A*) by presenting an intrasaccadic target step equal to the visual error vector (green arrow in Fig. 1 *A* and *B*). Because the adapt saccade vector and the visual error vector are in opposite directions, this combination produced a decrease in saccade size. Because the preferred bigger vector and the visual error vector are in same direction, this combination produced an increase in saccade size. To keep the vector of the postsaccadic visual error constant (green arrow in Fig. 1*B*) during the entire adaptation session, we used a modified version of the conventional McLaughlin paradigm (20, 39, 50, 74). As the monkey made a saccade toward the target, we measured the eye position at the end of the saccade (determined when eye velocity fell to 20°/s) and moved the target relative to that measured eye position by a constant visual error vector (Fig. 1*B*, late adaptation). Maintaining a constant visual error was crucial for this inactivation experiment. Had we used the original McLaughlin paradigm, the error size would have decreased during the adaptation, and the area representing the ever-decreasing visual error would have drifted rostrally on the SC out of the inactivated area. By maintaining a constant error, the SC injection site always represented the visual error during adaptation (green arrow in Fig. 1*A*). The muscimol injection did not affect the metrics of saccades in the adapt saccade vector (see *Results* for detail). On the other hand, the injection reduced the amplitude of the preferred bigger vector saccade in half of experiments. Because we cannot conclude whether such a gain change is induced by adaptation or the direct effect of muscimol on the amplitude of the saccade to the preferred bigger vector, we excluded the three with reduced amplitudes in the gain increase experiments from the further analysis.

Two days after the inactivation experiment, the dysmetria had completely disappeared, and we then collected behavioral control adaptations on each of

the next 3 d. We started the control adaptation after the monkey had made about the same number of preinjection and postinjection trials for the same amount of time as it did in the injection experiment. The adaptation was induced using the same vectors as in the injection experiment. A complete dataset comprises one injection experiment and the three associated behavioral controls.

Data Analysis. We digitized eye and target position signals at 1 kHz and sampled unit activity at 50 kHz using Power 1401 data acquisition/controller hardware (Cambridge Electronic Design). We saved data to a hard disk for later analysis. During the experiment, a custom program running in Spike2 (Cambridge Electronic Design) controlled the target movement and the monkey's reward via the Power 1401 hardware.

We used a custom program running in Spike2 to analyze the saved data. It detected saccades when eye velocity exceeded 75°/s within 50–800 ms after a target jump. The program marked saccade onset and end when the vector eye velocity exceeded or fell below a 20°/s threshold, respectively. The program measured several saccade attributes, e.g., amplitude, peak velocity, and duration, as well as the distance to the target at the beginning of each saccade. We exported saccade attributes and target positions to MATLAB (MathWorks) to analyze their relationships. We eliminated saccades whose initial eye positions differed from those of the initial target positions by >5°.

As reported previously (44), nystagmus (contraversive slow phase) appeared about a half hour after the injection. This most likely is caused by the spread of muscimol to the nucleus of the optic tract, which is located immediately rostral to the SC (44, 52–54). Because nystagmus may affect adaptation, we only analyzed saccades that were made before the nystagmus appeared. *SI Appendix*, Fig. S1*A*, shows data from a representative experiment in which muscimol was injected into the right SC (Exp 1, Table 1). There was no nystagmus before the injection (*SI Appendix*, Fig. S1*A*, time 1) so the eye velocity during fixation (yellow arrow) was ∼0°/s (cyan dashed line). Twenty-five minutes after the injection at the beginning of the adaptation block, the eye velocity was still ∼0°/s (*SI Appendix*, Fig. S1*A*, time 2). Thirty-five minutes later, nystagmus with a leftward slow-phase appeared so the eye velocity (yellow arrow) during fixation was slightly less than 0°/s (cyan dashed line; *SI Appendix*, Fig. S1*A*, time 3). The velocity of the nystagmus continued to increase for up to 1 h after the injection (*SI Appendix*, Fig. S1*A*, times 4 and 5).

To determine when to end the analysis, we calculated the average eye velocity between 20 and 50 ms before the onset of each saccade. We determined the time when the moving average of a 25-saccade trial window exceeded ±2°/s (*SI Appendix*, Fig. S1*B*, gray horizontal dashed line labeled "2°/s"). In this experiment, it occurred at 2,127 s (gray vertical dashed line labeled "Time to end Analysis," *SI Appendix*, Fig. S1*B*). *SI Appendix*, Fig. S1*C*, shows an experiment from the other monkey (Exp 6, Table 1). Here the muscimol was injected into the left SC so the slow phase of the nystagmus was rightward. The eye velocity of the slow phase exceeded 2°/s after only 1,205 s, much sooner than in *SI Appendix*, Fig. S1*B*. Because this latter injection was more rostral than that of *SI Appendix*, Fig. S1*B* (optimal amplitude was 2.3° vs. 6°, respectively; Table 1), the muscimol likely spread to the nucleus of the optic tract sooner.

After the muscimol injection, the monkey still made a corrective saccade corresponding to the intrasaccadic target step (*SI Appendix*, Fig. S1*A*). The reaction time of the corrective saccades was significantly longer in the injection experiments (median of six experiments = 348.1 ms) than in the control experiments (median of nine experiments = 186.2 ms) (Wilcoxon rank sum test, $P = 3.6 \times 10^{-4}$) (see also Fig. 2*B*).

To document saccade adaptation, we calculated the vector gain of each saccade. To account for trial-to-trial differences of initial eye position before a saccade, the target step size was computed relative to the initial eye position.

$$\text{Gain} = \frac{\sqrt{(\text{horizontal initial eye position} - \text{horizontal end eye position})^2 + (\text{vertical initial eye position} - \text{vertical end eye position})^2}}{\sqrt{(\text{horizontal initial eye position-horizontal target end position})^2 + (\text{vertical initial eye position} - \text{vertical target end position})^2}}.$$

Because the total number of trials differed in the injection and behavioral control experiments, we analyzed only the same number of trials in each of the four experiments in a dataset; that number was the fewest saccades in one of the four experiments.

To compare the progression of adaptation between the injection and control experiments (e.g., Fig. 4), we fitted the course of each adaptation with an exponential function:

$$f(x) = a \times \exp(-b \times x) + c.$$

We tested whether an injection experiment and a control experiment produced different exponential fits by means of an overall F test for regression (75). Briefly, the null hypothesis is that one exponential fits all of the data points from both the injection and control datasets. The alternative hypothesis is that the fits are different. The F ratio is the ratio between the percent difference of the sum-of-squares of errors from the null hypothesis and the sum of the two sums-of-squares of errors from the two alternative hypotheses fits (injection vs. combined data points and control vs. combined data points) and the percent difference in their degree of freedom. If the null hypothesis is true, the F ratio is 1.0. We then computed a P value from the F distribution. When $P < 0.05$, we consider that the data from the injection and each control experiment were significantly different.

We also calculated the amount of gain change in the injection and each control experiment (e.g., Fig. 5):

$$\text{Amount of gain change} = \text{median gain of the last 25 saccades} - \text{median gain of the first 25 saccades.}$$

To test whether the gain change was significant, we used a Wilcoxon rank sum test. If $P < 0.05$, we consider that the gain change was significant.

The datasets of this study are available at https://drive.google.com/open?id=1UpeP6u6bFo-JjN3FKh63BHIVUoZY7rFd.

ACKNOWLEDGMENTS. This study was supported by National Institute of Health (NIH) Grants EY023277 (R01 for Y.K.), EY019258 (R01 for R.S.), OD010425 (P51 for Washington National Primate Research Center), Vision Research Core (P30EY001730 for UW), and National Science Foundation BCS-1724176. The contents of this paper are solely the responsibility of the authors and do not necessarily represent the official views of National Center for Research Resources or NIH. Albert Fuchs helped with the editing.

1. Albus JS (1971) A theory of cerebellar function. *Math Biosci* 10:25–61.
2. Marr D (1969) A theory of cerebellar cortex. *J Physiol* 202:437–470.
3. Ito M (2005) Bases and implications of learning in the cerebellum—Adaptive control and internal model mechanism. *Prog Brain Res* 148:95–109.
4. Demer JL, Robinson DA (1982) Effects of reversible lesions and stimulation of olivocerebellar system on vestibuloocular reflex plasticity. *J Neurophysiol* 47: 1084–1107.
5. de'Sperati C, Lopiano L, Montarolo PG (1989) Lesions of the inferior olive do not affect long- or short-term habituation of the acoustic startle response in rats. *Neurosci Lett* 100:164–168.
6. Haddad GM, Demer JL, Robinson DA (1980) The effect of lesions of the dorsal cap of the inferior olive on the vestibulo-ocular and optokinetic systems of the cat. *Brain Res* 185:265–275.
7. Llinás R, Walton K, Hillman DE, Sotelo C (1975) Inferior olive: Its role in motor learing. *Science* 190:1230–1231.
8. Tempia F, Dieringer N, Strata P (1991) Adaptation and habituation of the vestibulo-ocular reflex in intact and inferior olive-lesioned rats. *Exp Brain Res* 86:568–578.
9. Kotajima H, Sakai K, Hashikawa T, Yanagihara D (2014) Effects of inferior olive lesion on fear-conditioned bradycardia. *Neuroreport* 25:556–561.
10. McCormick DA, Steinmetz JE, Thompson RF (1985) Lesions of the inferior olivary complex cause extinction of the classically conditioned eyeblink response. *Brain Res* 359:120–130.
11. Mintz M, Lavond DG, Zhang AA, Yun Y, Thompson RF (1994) Unilateral inferior olive NMDA lesion leads to unilateral deficit in acquisition and retention of eyelid classical conditioning. *Behav Neural Biol* 61:218–224.
12. Türker KS, Miles TS (1986) Climbing fiber lesions disrupt conditioning of the nictitating membrane response in the rabbit. *Brain Res* 363:376–378.
13. Voneida TJ, Christie D, Bogdanski R, Chopko B (1990) Changes in instrumentally and classically conditioned limb-flexion responses following inferior olivary lesions and olivocerebellar tractotomy in the cat. *J Neurosci* 10:3583–3593.
14. Welsh JP, Harvey JA (1998) Acute inactivation of the inferior olive blocks associative learning. *Eur J Neurosci* 10:3321–3332.
15. Yeo CH, Hardiman MJ, Glickstein M (1986) Classical conditioning of the nictitating membrane response of the rabbit. IV. Lesions of the inferior olive. *Exp Brain Res* 63:81–92.

16. Yakushin SB, Reisine H, Büttner-Ennever J, Raphan T, Cohen B (2000) Functions of the nucleus of the optic tract (NOT). I. Adaptation of the gain of the horizontal vestibulo-ocular reflex. *Exp Brain Res* 131:416–432.
17. Carrel AJ, Zenitsky GD, Bracha V (2013) Blocking glutamate-mediated inferior olivary signals abolishes expression of conditioned eyeblinks but does not prevent their acquisition. *J Neurosci* 33:9097–9103.
18. Ke MC, Guo CC, Raymond JL (2009) Elimination of climbing fiber instructive signals during motor learning. *Nat Neurosci* 12:1171–1179.
19. Scudder CA, Kaneko CS, Fuchs AF (2002) The brainstem burst generator for saccadic eye movements: A modern synthesis. *Exp Brain Res* 142:439–462.
20. McLaughlin S (1967) Parametric adjustment in saccadic eye movements. *Percept Psychophys* 2:359–362.
21. Straube A, Deubel H, Ditterich J, Eggert T (2001) Cerebellar lesions impair rapid saccade amplitude adaptation. *Neurology* 57:2105–2108.
22. Waespe W, Baumgartner R (1992) Enduring dysmetria and impaired gain adaptivity of saccadic eye movements in Wallenberg's lateral medullary syndrome. *Brain* 115: 1123–1146.
23. Barash S, et al. (1999) Saccadic dysmetria and adaptation after lesions of the cerebellar cortex. *J Neurosci* 19:10931–10939.
24. Kojima Y, Soetedjo R, Fuchs AF (2011) Effect of inactivation and disinhibition of the oculomotor vermis on saccade adaptation. *Brain Res* 1401:30–39.
25. Takagi M, Zee DS, Tamargo RJ (1998) Effects of lesions of the oculomotor vermis on eye movements in primate: Saccades. *J Neurophysiol* 80:1911–1931.
26. Optican LM, Robinson DA (1980) Cerebellar-dependent adaptive control of primate saccadic system. *J Neurophysiol* 44:1058–1076.
27. Kojima Y, Soetedjo R, Fuchs AF (2010) Changes in simple spike activity of some Purkinje cells in the oculomotor vermis during saccade adaptation are appropriate to participate in motor learning. *J Neurosci* 30:3715–3727.
28. Soetedjo R, Fuchs AF (2006) Complex spike activity of purkinje cells in the oculomotor vermis during behavioral adaptation of monkey saccades. *J Neurosci* 26:7741–7755.
29. Soetedjo R, Kojima Y, Fuchs AF (2008) Complex spike activity in the oculomotor vermis of the cerebellum: A vectorial error signal for saccade motor learning? *J Neurophysiol* 100:1949–1966.
30. Soetedjo R, Kojima Y, Fuchs A (2008) Complex spike activity signals the direction and size of dysmetric saccade errors. *Prog Brain Res* 171:153–159.
31. Catz N, Dicke PW, Thier P (2005) Cerebellar complex spike firing is suitable to induce as well as to stabilize motor learning. *Curr Biol* 15:2179–2189.
32. Catz N, Dicke PW, Thier P (2008) Cerebellar-dependent motor learning is based on pruning a Purkinje cell population response. *Proc Natl Acad Sci USA* 105:7309–7314.
33. Kralj-Hans I, Baizer JS, Swales C, Glickstein M (2007) Independent roles for the dorsal paraflocculus and vermal lobule VII of the cerebellum in visuomotor coordination. *Exp Brain Res* 177:209–222.
34. Yamada J, Noda H (1987) Afferent and efferent connections of the oculomotor cerebellar vermis in the macaque monkey. *J Comp Neurol* 265:224–241.
35. Harting JK (1977) Descending pathways from the superior collicullus: An autoradiographic analysis in the rhesus monkey (Macaca mulatta). *J Comp Neurol* 173:583–612.
36. Huerta MF, Harting JK (1984) The mammalian superior colliculus studies of its morphology and connections. *Comparative Neurology of the Optic Tectum*, ed Vanegas H (Plenum Press, New York), pp 687–773.
37. Kaku Y, Yoshida K, Iwamoto Y (2009) Learning signals from the superior colliculus for adaptation of saccadic eye movements in the monkey. *J Neurosci* 29:5266–5275.
38. Soetedjo R, Fuchs AF, Kojima Y (2009) Subthreshold activation of the superior colliculus drives saccade motor learning. *J Neurosci* 29:15213–15222.
39. Kojima Y, Soetedjo R (2017) Change in sensitivity to visual error in superior colliculus during saccade adaptation. *Sci Rep* 7:9566.
40. Robinson DA (1972) Eye movements evoked by collicular stimulation in the alert monkey. *Vision Res* 12:1795–1808.
41. Quaia C, Aizawa H, Optican LM, Wurtz RH (1998) Reversible inactivation of monkey superior colliculus. II. Maps of saccadic deficits. *J Neurophysiol* 79:2097–2110.
42. Hikosaka O, Wurtz RH (1985) Modification of saccadic eye movements by GABA-related substances. I. Effect of muscimol and bicuculline in monkey superior colliculus. *J Neurophysiol* 53:266–291.
43. Munoz DP, Wurtz RH (1992) Role of the rostral superior colliculus in active visual fixation and execution of express saccades. *J Neurophysiol* 67:1000–1002.
44. Munoz DP, Wurtz RH (1993) Fixation cells in monkey superior colliculus. II. Reversible activation and deactivation. *J Neurophysiol* 70:576–589.
45. Hikosaka O, Wurtz RH (1983) Effects on eye movements of a GABA agonist and antagonist injected into monkey superior colliculus. *Brain Res* 272:368–372.
46. Straube A, Fuchs AF, Usher S, Robinson FR (1997) Characteristics of saccadic gain adaptation in rhesus macaques. *J Neurophysiol* 77:874–895.
47. Becker W (1989) The neurobiology of saccadic eye movements. Metrics. *Rev Oculomot Res* 3:13–67.
48. Hopp JJ, Fuchs AF (2004) The characteristics and neuronal substrate of saccadic eye movement plasticity. *Prog Neurobiol* 72:27–53.
49. Iwamoto Y, Kaku Y (2010) Saccade adaptation as a model of learning in voluntary movements. *Exp Brain Res* 204:145–162.
50. Kojima Y, Fuchs AF, Soetedjo R (2015) Adaptation and adaptation transfer characteristics of five different saccade types in the monkey. *J Neurophysiol* 114:125–137.
51. Hopp JJ, Fuchs AF (2002) Investigating the site of human saccadic adaptation with express and targeting saccades. *Exp Brain Res* 144:538–548.
52. Mustari MJ, Fuchs AF (1990) Discharge patterns of neurons in the pretectal nucleus of the optic tract (NOT) in the behaving primate. *J Neurophysiol* 64:77–90.
53. Schiff D, Cohen B, Büttner-Ennever J, Matsuo V (1990) Effects of lesions of the nucleus of the optic tract on optokinetic nystagmus and after-nystagmus in the monkey. *Exp Brain Res* 79:225–239.
54. Schiff D, Cohen B, Raphan T (1988) Nystagmus induced by stimulation of the nucleus of the optic tract in the monkey. *Exp Brain Res* 70:1–14.
55. Frens MA, Van Opstal AJ (1997) Monkey superior colliculus activity during short-term saccadic adaptation. *Brain Res Bull* 43:473–483.
56. Quessy S, Quinet J, Freedman EG (2010) The locus of motor activity in the superior colliculus of the rhesus monkey is unaltered during saccadic adaptation. *J Neurosci* 30: 14235–14244.
57. Inaba N, Iwamoto Y, Yoshida K (2003) Changes in cerebellar fastigial burst activity related to saccadic gain adaptation in the monkey. *Neurosci Res* 46:359–368.
58. Scudder CA, McGee DM (2003) Adaptive modification of saccade size produces correlated changes in the discharges of fastigial nucleus neurons. *J Neurophysiol* 90: 1011–1026.
59. Kojima Y, Iwamoto Y, Robinson FR, Noto CT, Yoshida K (2008) Premotor inhibitory neurons carry signals related to saccade adaptation in the monkey. *J Neurophysiol* 99: 220–230.
60. Kojima Y, Robinson FR, Soetedjo R (2014) Cerebellar fastigial nucleus influence on ipsilateral abducens activity during saccades. *J Neurophysiol* 111:1553–1563.
61. Batini C, Billard JM, Daniel H (1985) Long term modification of cerebellar inhibition after inferior olive degeneration. *Exp Brain Res* 59:404–409.
62. Colin F, Manil J, Desclin JC (1980) The olivocerebellar system. I. Delayed and slow inhibitory effects: An overlooked salient feature of cerebellar climbing fibers. *Brain Res* 187:3–27.
63. Montarolo PG, Palestini M, Strata P (1982) The inhibitory effect of the olivocerebellar input on the cerebellar Purkinje cells in the rat. *J Physiol* 332:187–202.
64. Medina JF, Nores WL, Mauk MD (2002) Inhibition of climbing fibres is a signal for the extinction of conditioned eyelid responses. *Nature* 416:330–333.
65. Zbarska S, Bloedel JR, Bracha V (2008) Cerebellar dysfunction explains the extinction-like abolition of conditioned eyeblinks after NBQX injections in the inferior olive. *J Neurosci* 28:10–20.
66. Zbarska S, Bracha V (2012) Assessing the role of inferior olivary sensory signaling in the expression of conditioned eyeblinks using a combined glutamate/GABAA receptor antagonist protocol. *J Neurophysiol* 107:273–282.
67. Judge SJ, Richmond BJ, Chu FC (1980) Implantation of magnetic search coils for measurement of eye position: An improved method. *Vision Res* 20:535–538.
68. Fuchs AF, Robinson DA (1966) A method for measuring horizontal and vertical eye movement chronically in the monkey. *J Appl Physiol* 21:1068–1070.
69. Munoz DP, Wurtz RH (1995) Saccade-related activity in monkey superior colliculus. I. Characteristics of burst and buildup cells. *J Neurophysiol* 73:2313–2333.
70. Sparks DL, Mays LE (1980) Movement fields of saccade-related burst neurons in the monkey superior colliculus. *Brain Res* 190:39–50.
71. National Research Council (2011) *Guide for the Care and Use of Laboratory Animals* (National Academies Press, Washington, DC), 8th Ed.
72. Soetedjo R, Kaneko CR, Fuchs AF (2002) Evidence that the superior colliculus participates in the feedback control of saccadic eye movements. *J Neurophysiol* 87:679–695.
73. Soetedjo R, Kaneko CR, Fuchs AF (2002) Evidence against a moving hill in the superior colliculus during saccadic eye movements in the monkey. *J Neurophysiol* 87: 2778–2789.
74. Robinson FR, Noto CT, Bevans SE (2003) Effect of visual error size on saccade adaptation in monkey. *J Neurophysiol* 90:1235–1244.
75. Motulsky H, Christopoulos A (2004) Using global fitting to test a treatment effect in one experiment. *Fitting Models to Biological Data Using Linear and Nonlinear Regression: A Practical Guide to Curve Fitting* (Oxford Univ Press, New York), 1st Ed, pp 163–165.